

Unambiguously Testing Positivity at Lepton Colliders

Jiayin Gu,^{1,2,3,*} Lian-Tao Wang,^{4,5,†} and Cen Zhang^{6,7,‡}

¹*Department of Physics and Center for Field Theory and Particle Physics, Fudan University, Shanghai 200438, China*

²*Key Laboratory of Nuclear Physics and Ion-beam Application (MOE), Fudan University, Shanghai 200433, China*

³*PRISMA⁺ Cluster of Excellence, Institut für Physik,*

Johannes Gutenberg-Universität, Staudingerweg 7, 55128 Mainz, Germany

⁴*Department of Physics and Enrico Fermi Institute, University of Chicago, Chicago, IL 60637, USA*

⁵*Kavli Institute for Cosmological Physics, University of Chicago, Chicago, IL 60637, USA*

⁶*Institute for High Energy Physics, and School of Physical Sciences,*
University of Chinese Academy of Sciences, Beijing 100049, China

⁷*Center for High Energy Physics, Peking University, Beijing 100871, China*

The diphoton channel at lepton colliders, $e^+e^-(\mu^+\mu^-) \rightarrow \gamma\gamma$, has a remarkable feature that the leading new physics contribution comes only from dimension-eight operators. This contribution is subject to a set of positivity bounds, derived from the fundamental principles of Quantum Field Theory, such as unitarity, locality, analyticity and Lorentz invariance. These positivity bounds are thus applicable to the most direct observable — the diphoton cross section. This unique feature provides a clear, robust, and unambiguous test of these principles. We estimate the capability of various future lepton colliders in probing the dimension-eight operators and testing the positivity bounds in this channel. We show that positivity bounds can lift certain flat directions among the effective operators and significantly change the perspectives of a global analysis. We also discuss the positivity bounds of the $Z\gamma/ZZ$ processes which are related to the $\gamma\gamma$ ones, but are more complicated due to the massive Z boson.

In memory of Cen Zhang

Introduction.— Positivity bounds on coefficients for operators in the Standard Model Effective Field Theory (SMEFT) arise from the assumption that their UV completion obeys the fundamental principles of quantum field theory (QFT), such as unitarity, locality, analyticity and Lorentz invariance. Testing these bounds at colliders is difficult, as they generally only apply to effects of dimension-eight (dim-8) or higher operators [1–13]. Their contribution to a given process is typically subleading compared with those from dimension-six (dim-6) operators, making their measurements experimentally challenging even with differential observables [12, 14]. For dim-6 operators, such bounds do not exist without explicit assumptions on the UV model [15–19].

In this letter, we identify a specific process, $e^+e^- \rightarrow \gamma\gamma$ (or $\mu^+\mu^- \rightarrow \gamma\gamma$), in which the dim-8 operators provide the leading new physics contribution, and a test of the positivity bounds can be unambiguously carried out. The measurements of this simple process at lepton colliders thus have profound implications. A confirmed violation of the positivity bounds would be more revolutionary than any particle discovery, as it would indicate a breakdown of at least one of the foundations of QFT.

The diphoton channel.— The leading new physics contributions to $e^+e^- \rightarrow \gamma\gamma$ appear at dim-8. This can be easily deduced in the massless tree-level limit as follows, and we postpone a more detailed discussion of the dim-6 effects to the next section. Neglecting the electron mass, the tree-level SM amplitude takes only the $\mathcal{A}(f^+f^-\gamma^+\gamma^-)$ helicity configuration (the superscripts

denote the helicity), where $f = e_{L,R}$ is the left- or right-handed electron. The lowest order new physics contribution to the same helicity amplitude (required to generate an interference term with the SM) is a contact interaction that has mass dimension four, which is generated by dim-8 operators. Denoting with e the electric coupling, v the Higgs vacuum expectation value (vev), the amplitude of the diphoton process can be written as

$$\begin{aligned} & \mathcal{A}(f^+f^-\gamma^+\gamma^-)_{\text{SM+d8}} \\ &= 2e^2 \frac{\langle 24 \rangle^2}{\langle 13 \rangle \langle 23 \rangle} + \frac{a}{v^4} [13][23]\langle 24 \rangle^2 \\ &= 2e^2 \frac{\langle 24 \rangle^2}{\langle 13 \rangle \langle 23 \rangle} \left(1 + \frac{a}{2e^2 v^4} tu \right), \end{aligned} \quad (1)$$

where the effective parameter a (denoted as $a_{L,R}$ later for $f = e_{L,R}$) depends on the dim-8 coefficients, and s, t, u are the Mandelstam variables. Here we only highlight the key features of the helicity amplitude formalism used in Eq. (1) and refer the readers to recent reviews [20–22] for more details. The two-component spinor $|p\rangle$ ($|p\rangle$) has mass dimension 1/2 and helicity +1/2 (−1/2). The total helicities of the amplitude need to be consistent with the ones of the external particles (labelled in numerical order). This uniquely fixes the form of the dim-8 contact term, which has an overall mass dimension of four, while $[13]^2\langle 14 \rangle \langle 24 \rangle = -[13][23]\langle 24 \rangle^2$ is not independent. A contact term with a lower mass dimension could not be written down for the same helicity amplitude. We note here that, by definition, a positive a indicates a construc-

tive interference between the SM and the dim-8 amplitudes.

Positivity bounds can be derived from a twice-subtracted dispersion relation, assuming that the UV completion obeys the fundamental principles of QFT [1]. The dispersion relation connects the second s derivative of an elastic amplitude to an integration of its discontinuity, which is positive definite. Rotating the diphoton amplitude to the elastic process $e\gamma \rightarrow e\gamma$, and taking the forward limit, we have

$$\begin{aligned} \mathcal{A}(f^+\gamma^+f^-\gamma^-)_{\text{SM+d8}} &= 2e^2 \frac{\langle 34 \rangle^2}{\langle 12 \rangle \langle 32 \rangle} \left(1 + \frac{a}{2e^2 v^4} su \right) \\ &\stackrel{t \rightarrow 0}{=} \mathcal{M}_{\text{SM}} \left(1 - \frac{a}{2e^2 v^4} s^2 \right), \end{aligned} \quad (2)$$

where $\mathcal{M}_{\text{SM}} \equiv 2e^2 \frac{\langle 34 \rangle^2}{\langle 12 \rangle \langle 32 \rangle} |_{t \rightarrow 0}$ is the SM amplitude in the forward limit. An important feature of the $e\gamma \rightarrow e\gamma$ process is that, in the forward limit where the positivity bound is derived, the SM amplitude is a nonzero finite constant, and one could explicitly show that (see Appendix A) $\mathcal{M}_{\text{SM}} = -2e^2$. This is in contrast with the examples in Ref. [1], where the dim-4 Lagrangian is a free theory and the interference term does not exist. In other cases (such as the scattering of two fermions), the SM elastic amplitude may have a t -channel pole from the exchange of a massless particle, and the forward limit is not well defined. In such cases, additional treatments are needed to obtain meaningful positivity bounds, for instance by systematically subtracting all calculable SM contributions to the amplitude before taking the forward limit. It is also possible for the SM amplitude to have s -channel poles that may contaminate the positivity bounds of dim-8 coefficients, which again need to be systematically subtracted. These cases introduce additional steps and subtleties in understanding the implications of positivity bounds on observables. The fact that the SM $e\gamma \rightarrow e\gamma$ forward amplitude is a finite constant means that the positivity bound also uniquely fixes the relative sign of the SM and dim-8 contributions, as suggested by Equation 2. Due to crossing, a positive a here corresponds to a destructive interference between the SM and dim-8 terms. Since $\mathcal{M}_{\text{SM}} = -2e^2 < 0$, the positivity bound,

$$\frac{d^2}{ds^2} \mathcal{A}(f^+\gamma^+f^-\gamma^-)|_{t \rightarrow 0} \geq 0, \quad (3)$$

implies $a \geq 0$. The interference between SM and dim-8 contributions is thus bounded to be destructive in $e\gamma \rightarrow e\gamma$, and **constructive** in $e^+e^- \rightarrow \gamma\gamma$.

One could work in the *amplitude basis* [23, 24] and directly connect Eq. (1) with the massless amplitudes of the W and B fields in the unbroken electroweak phase. Alternatively, using the basis of Ref. [25] (see also Ref. [26]), a_L and a_R are given by

$$a_L = -2 \frac{v^4}{\Lambda^4} \left(c_W^2 c_{l^2 B^2 D} - 2s_W c_W c_{l^2 W B D}^{(2)} + s_W^2 c_{l^2 W^2 D}^{(1)} \right),$$

$$a_R = -2 \frac{v^4}{\Lambda^4} \left(c_W^2 c_{e^2 B^2 D} + s_W^2 c_{e^2 W^2 D} \right), \quad (4)$$

where $s_W \equiv \sin \theta_W$, $c_W \equiv \cos \theta_W$, c_i 's are the coefficients of the five dim-8 operators, Q_i , as defined in Ref. [25] (see Appendix A), and Λ denotes the scale of the potential new physics. They are the only relevant operators in the full dim-8 basis, not only for diphoton but also for the CP-even $\mathcal{A}(\bar{e}_L e_L V_1^+ V_2^-)_{\text{d8}}$ and $\mathcal{A}(e_R \bar{e}_R V_1^+ V_2^-)_{\text{d8}}$ amplitudes in the massless limit, where $V_{1,2} = Z, \gamma$.

Dim-6 contributions.— A dim-6 tree-level contribution to the diphoton process can be generated only by a dipole operator, and has a different fermion helicity configuration than the SM one, $\mathcal{A}(f^+f^-\gamma^+\gamma^-)$. The dim-6 interference term therefore does not exist [27]. At the one-loop level, several dim-6 contributions arise, but they are all strongly constrained by other measurements, and can be safely ignored with a loop factor suppression. For instance, operator $\mathcal{O}_{3W} = \frac{1}{3!} g \epsilon_{abc} W_\mu^{a\nu} W_{\nu\rho}^b W^{c\rho\mu}$ contributes to $\mathcal{A}(f^+f^-\gamma^+\gamma^-)$ at one loop, but it can be very-well probed by the $e^+e^- \rightarrow WW$ process. A rough estimation with the projections from Ref. [28] ($\lesssim 10^{-4}$ in terms of the anomalous triple-gauge couplings) suggests that its impact on the diphoton cross section is at most around $\delta\sigma_{\gamma\gamma}/\sigma_{\gamma\gamma} \sim 10^{-7}$, much smaller than the expected precision at a realistic lepton collider (see Appendix A). Similarly, the modifications in the $Ze^+e^- (Z\mu^+\mu^-)$ couplings are already stringently constrained at the 10^{-4} (10^{-3}) level even with current measurements [28], and their loop contributions to the diphoton process can be safely neglected. The one loop contributions involving the Higgs boson are also irrelevant since they are suppressed by the square of electron (muon) Yukawa coupling. While the four-fermion operators involving two electrons and two top-quark fields are poorly constrained, their contribution to $\mathcal{A}(f^+f^-\gamma^+\gamma^-)$ is forbidden by the angular momentum selection rules, since they cannot produce the $J = 2$ state of two photons [29]. The interference between the one-loop SM amplitude and the tree-level dipole contribution is also absent with massless electrons. Contributions with two insertions of dim-6 operators are formally indistinguishable from dim-8 operators. At the tree level, the only such contribution which is not equivalent to a contact dim-8 operator insertion comes from two insertions of electron dipole couplings¹. They are strongly constrained by the $g_e - 2$ and the electric dipole moment measurements [31, 32]. A rough estimation suggests that their impact on the diphoton cross section is at most $\frac{\delta\sigma_{\gamma\gamma}}{\sigma_{\gamma\gamma}} \sim \left(\frac{E}{10^7 \text{TeV}}\right)^2$ where E is the center-of-mass energy, and can be safely ignored. Finally, we note that dim-8 operators involving Higgs

¹ One could always choose a basis, such as the Warsaw basis [30], in which the only dim-6-squared contribution comes from the dipole operators.

fields do not contribute to $\mathcal{A}(f^+f^-\gamma^+\gamma^-)$ either, as the insertion of a Higgs vev makes the amplitude effectively at a lower mass dimension, where a contact term for $\mathcal{A}(f^+f^-\gamma^+\gamma^-)$ does not exist.

Naively, one expects that the dim-6 contributions from new physics will be first observed in some other processes. What then is the motivation to look for dim-8 deviations in $e^+e^- \rightarrow \gamma\gamma$? First, testing positivity at dim-8 provides more fundamental information about the nature of new physics, namely whether it is consistent with the QFT framework, which one cannot tell from a SMEFT analysis truncated at dim-6. An observation of dim-6 deviation elsewhere would only strengthen the motivation to test dim-8 deviations in $e^+e^- \rightarrow \gamma\gamma$. Second, dim-6 effects from different UV states could be suppressed due to dynamics [33], certain symmetries [18], or accidental cancellation. In contrast, constraining the positively bounded dim-8 effects could lead to unambiguous exclusion limits on all possible UV particles, as each of them contributes positively, assuming the QFT framework is valid [12].

Positivity bounds on cross sections.— The positivity bounds, $a_L \geq 0$ and $a_R \geq 0$, restrict the interference between SM and dim-8 contributions to be constructive in $e^+e^- \rightarrow \gamma\gamma$. As such, they can be directly related to the cross section. Since the helicities of the two photons cannot be measured in practice, we work with the folded distribution of the production polar angle θ ,

$$\begin{aligned} & \frac{d\sigma(e^+e^- \rightarrow \gamma\gamma)}{d|\cos\theta|} \\ &= \frac{(1 - P_{e^-})(1 + P_{e^+})}{4} \frac{e^4}{4\pi s} \left(\frac{1 + c_\theta^2}{1 - c_\theta^2} + a_L \frac{s^2(1 + c_\theta^2)}{4e^2v^4} \right) \\ &+ \frac{(1 + P_{e^-})(1 - P_{e^+})}{4} \frac{e^4}{4\pi s} \left(\frac{1 + c_\theta^2}{1 - c_\theta^2} + a_R \frac{s^2(1 + c_\theta^2)}{4e^2v^4} \right), \end{aligned} \quad (5)$$

where s is the square of the center-of-mass energy, P_{e^-} (P_{e^+}) is the polarization of the electron (positron) beam, and $c_\theta \equiv |\cos\theta|$. The a_L , a_R terms come from the interference between SM and dim-8 operators, while the dim-8-squared contributions can be safely neglected due to the high measurement precision of this channel at lepton colliders. It is now clear that the positivity bounds $a_L \geq 0$, $a_R \geq 0$ have a simple consequence, namely

$$\frac{d\sigma}{d|\cos\theta|}(e^+e^- \rightarrow \gamma\gamma) \geq \frac{d\sigma_{\text{SM}}}{d|\cos\theta|}(e^+e^- \rightarrow \gamma\gamma), \quad (6)$$

for any beam polarizations and any $|\cos\theta|$. We see that the $e^+e^- \rightarrow \gamma\gamma$ channel is special in that the positivity of Wilson coefficients can be directly translated into positivity in realistic observables, without being contaminated by any other non-positive operators. The diphoton process thus provides a simple, clear, and unambiguous test of the fundamental principles of QFT.

It is also interesting to note that the measurements at LEP2 display an overall signal strength of $e^+e^- \rightarrow \gamma\gamma$ to be about 1.5 standard deviations below the SM expectation [34]. While statistically insignificant, this deviation exhibits a small tension with the positivity bound.

Collider reach.— To estimate the reach at future lepton colliders, we perform a simple binned analysis in the range $|\cos\theta| \in [0, 0.95]$, with a bin width of 0.05, and consider only statistical uncertainties. A differential analysis in $|\cos\theta|$ helps discriminate the dim-8 contribution from the SM one, as the latter dominates the forward region due to the t/u -channel electron exchange. We expect the largest background to be the Bhabha scattering ($e^+e^- \rightarrow e^+e^-$). Assuming a sufficiently small rate ($\ll 1\%$) for an electron to be misidentified as a photon, this background is more than two orders of magnitude smaller than the signal (see Appendix A). The cut on the minimal production polar angle ($|\cos\theta| < 0.95$) is also very effective in removing the beamstrahlung and ISR effects. We note that the reach on Λ is only mildly sensitive to the measurement uncertainties ($\sim \Delta^{-1/4}$) due to the $1/\Lambda^4$ dependence of the dim-8 contribution, so our analysis gives a reasonable projection as long as the systematic uncertainties are not overwhelmingly large. As a validation, we apply it to the LEP2 run scenarios and find a very good agreement with the result of Ref. [34] (with a $\lesssim 10\%$ difference in the reach on Λ).

To illustrate the interplay between the measurements and the positivity bounds, we show the $\Delta\chi^2 = 1$ contours in Figure 1 for collider scenarios CEPC/FCC-ee 240 GeV [35–37] and ILC 250 GeV [38]. According to Eq. (5), if the beams are unpolarized ($P_{e^-} = P_{e^+} = 0$), only the combination $a_L + a_R$ is probed, leaving a flat direction along $a_L = -a_R$ as shown by the diagonal band (indicating $\Delta\chi^2 \leq 1$) for CEPC/FCC-ee. It can be lifted by having multiple runs with different beam polarization, as for example at the ILC. Clearly, beam polarization is desirable, because it allows for testing the signs of a_L and a_R (or the two polarized cross sections) individually.

On a different ground, assuming the UV completion is consistent with the QFT principles which imply $a_L, a_R \geq 0$, a_L and a_R can be simultaneously constrained even without beam polarization, as illustrated in Figure 1. This is a general feature that also applies to many other processes, such as the fermion scattering [12] or the Higgs production [39]. Positivity thus provides important information for future global SMEFT analyses, complementary to the experimental inputs.

High energy lepton colliders can probe these operators even further. The precision reach on the parameter a scales with the energy E and luminosity L as $\Delta a \sim E^{-3}L^{-1/2}$, as the energy dependence of the dim-8 contribution gives an E^{-4} dependence, and the measurement uncertainties are proportional to $(\sigma_{\text{SM}} \cdot L)^{-1/2} \sim$

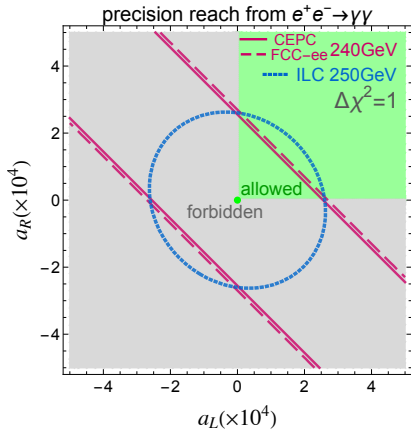


FIG. 1: $\Delta\chi^2 = 1$ contours for CEPC/FCC-ee 240 GeV and ILC 250 GeV. The green shaded region is allowed by the positivity bounds.

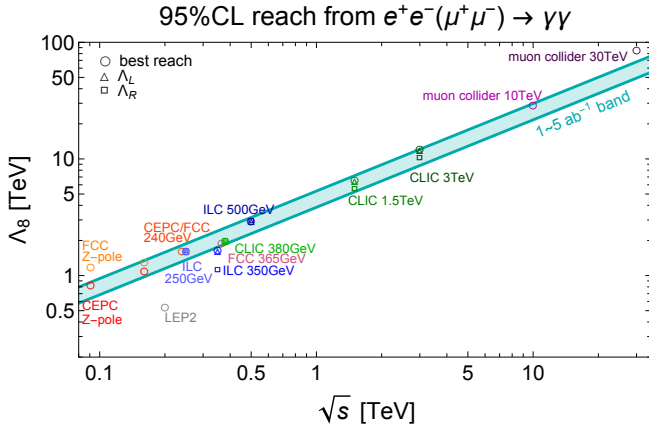


FIG. 2: The reach on the scale of the dim-8 operators $\Lambda_8 (\equiv v/a^{\frac{1}{4}})$ as a function of the center-of-mass energy \sqrt{s} from the measurement of the $e^+e^- \rightarrow \gamma\gamma$ (or $\mu^+\mu^- \rightarrow \gamma\gamma$) process. The band covers $1 - 5 \text{ ab}^{-1}$ and various beam polarization scenarios. The circle represents the best reach of each collider scenario. The LEP2 [34] reach is shown assuming a SM central value. For linear colliders, the triangle (square) shows the reach for a_L (a_R) in a simultaneous fit of both parameters. Note that the luminosities of FCC Z-pole (150 ab^{-1}), LEP2 (3 fb^{-1}) and muon collider 30 TeV (90 ab^{-1}) are all very different from the $1\text{-}5 \text{ ab}^{-1}$ of the band.

$E \cdot L^{-1/2}$. Since $a \sim 1/\Lambda^4$, the reach of Λ thus scales as

$$\frac{\Lambda_2}{\Lambda_1} = \left(\frac{E_2}{E_1}\right)^{\frac{3}{4}} \left(\frac{L_2}{L_1}\right)^{\frac{1}{8}}, \quad (7)$$

assuming all other variables are the same for the two scenarios 1 and 2.

In Figure 2, we show the 95% CL reach for $\Lambda_8 \equiv v/a^{\frac{1}{4}}$ for various collider scenarios, where $a = a_L, a_R$ is defined in Eqs. (1). Λ_8 corresponds directly to the scale of new physics which modifies the $e^+e^- \rightarrow \gamma\gamma$ amplitudes. The band covers integrated luminosities of 1 to

5 ab^{-1} and various beam polarization scenarios, and is consistent with Eq. (7). We also show the best reach for each collider scenario listed in Appendix A from any linear combinations of a_L and a_R . For linear colliders, a_L and a_R can be independently constrained, and the corresponding Λ_L and Λ_R are also shown.

Similar analyses can be carried out for muon colliders, which probe operators associated with muon fields. Constraints on muon dipole moments [32] are significantly weaker than those of the electron ones. We find that two insertions of the electric dipole operator could generate a deviation in the $\mu^+\mu^- \rightarrow \gamma\gamma$ cross section comparable to the expected precision reach. However, future improvements on the muon electric dipole moment measurement could make this contribution irrelevant ($\frac{\delta\sigma_{\gamma\gamma}}{\sigma_{\gamma\gamma}} \sim (\frac{E}{10^5 \text{ TeV}})^2$) [40, 41]. On the contrary, the current muon $g_\mu - 2$ measurement [42–44] sufficiently constrains the magnetic dipole operator, so that the latter can be safely ignored for the diphoton measurement ($\frac{\delta\sigma_{\gamma\gamma}}{\sigma_{\gamma\gamma}} \sim (\frac{E}{10^5 \text{ TeV}})^2$), independent of whether the apparent discrepancy with the SM is confirmed.

Interplay with $Z\gamma$ and ZZ measurements.— The same operators that enter Eq. (4) also contribute to the $Z\gamma$ and ZZ processes. These processes are, however, more complicated due to the massive Z boson, which enables contributions to multiple helicity states from both SM and dim-8 operators (including those responsible for neutral triple-gauge-boson couplings [45–48]). Dim-6 operators could also contribute at the tree level via modifications of the Ze^+e^- couplings. At very high energies ($\sqrt{s} \gg m_Z$), the Z boson is effectively massless, and the $+-$ final helicity states dominate the $Z\gamma$ and ZZ cross sections [7]. In this limit, the ZZ process also exhibits a similar positivity bound,

$$\frac{d\sigma}{d|\cos\theta|}(e^+e^- \rightarrow ZZ) \geq \frac{d\sigma_{\text{SM}}}{d|\cos\theta|}(e^+e^- \rightarrow ZZ). \quad (8)$$

For the $Z\gamma$ process, we focus on the CP-even elastic amplitude $\mathcal{A}(eV \rightarrow eV)$, where V is an arbitrarily mixed state of γ and Z . This gives

$$(a_L^{Z\gamma})^2 \leq a_L^{ZZ} a_L^{\gamma\gamma}, \quad (a_R^{Z\gamma})^2 \leq a_R^{ZZ} a_R^{\gamma\gamma}, \quad (9)$$

where $a_{L,R}^{Z\gamma}$ ($a_{L,R}^{ZZ}$) is defined as in Eq. (1) with $\gamma^+\gamma^-$ replaced by $Z^+\gamma^-$ (Z^+Z^-), together with $a_{L,R} \rightarrow a_{L,R}^{\gamma\gamma}$ to distinguish them. This implies a simple relation among the $Z\gamma$, $\gamma\gamma$ and ZZ cross sections for any fixed collider scenario (again only in the $\sqrt{s} \gg m_Z$ limit),

$$(\Delta\sigma_{Z\gamma})^2 \leq 4\Delta\sigma_{\gamma\gamma}\Delta\sigma_{ZZ}, \quad (10)$$

where $\Delta\sigma \equiv \frac{d\sigma}{d|\cos\theta|} - \frac{d\sigma_{\text{SM}}}{d|\cos\theta|}$. We note here again that a proper treatment of the $Z\gamma$ and ZZ processes requires the inclusion of all helicity states of the gauge bosons. The decay of the Z boson also provides new observables sensitive to the interference of different Z helicity

states [48–50]. The mapping between positivity bounds and observables in the $Z\gamma/ZZ$ processes are generally more complicated, and we leave such an analysis to future studies. On the contrary, the positivity bound of the diphoton process is simple and unambiguous, as we emphasized above.

Violation of positivity.— The observation of $\frac{d\sigma(e^+e^- \rightarrow \gamma\gamma)}{d|\cos\theta|} < \frac{d\sigma_{\text{SM}}(e^+e^- \rightarrow \gamma\gamma)}{d|\cos\theta|}$ does not necessarily establish the violation of positivity bounds. It is important to check whether the EFT description itself is invalid, for instance, due to contributions from new light particles. In this process, however, it is difficult for such particles to generate a sizable destructive interference term while evading the current and future search constraints. A t -channel fermion exchange only generates a constructive interference. Another possibility is an s -channel exchange of a light composite spin-2 particle, which could be very-well probed by the resonance search $e^+e^- \rightarrow X\gamma/XZ$, $X \rightarrow \gamma\gamma/e^+e^-$ [51]. Measuring the diphoton process at multiple center-of-mass energies also helps probe or exclude these light particle contributions and further verifies that the observed deviations are generated by dim-8 operators. After all other possibilities are excluded, the result would then indicate the breakdown of the fundamental principles of QFT². Interestingly, a recent study [52] shows with an explicit example that order-one violations of positivity bounds could be generated if the Lorentz symmetry is spontaneously broken.

Summary and outlook.— Positivity bounds require that the diphoton cross section at lepton colliders must be no smaller than the SM prediction, which offers a rare opportunity to clearly and unambiguously test the fundamental principles of QFT. While high energy colliders provide the best reaches, such probes are robust even for a collider at around 240-250 GeV, a feature that is unique for the diphoton process. Alternatively, imposing these bounds could lift the flat directions among operators, indicating that positivity could provide important information for future global analyses with dim-8 operators.

Hadron colliders, such as the LHC or a future 100-TeV collider, have a large center-of-mass energy and could potentially provide powerful probes on the dim-8 operators and their associated positivity bounds [7, 8, 14]. In particular, a similar process with quarks, $q\bar{q} \rightarrow \gamma\gamma$ (or $q\bar{q} \rightarrow Z\gamma/ZZ$ [7]), is already probed at the LHC with a larger center-of-mass energy than the ones of most future lepton colliders. However, these measurements usually suffer from low measurement precisions which make the EFT interpretation problematic, and a consistent EFT

treatment often results in much reduced sensitivities to the new physics scale [53, 54]. This is particularly important for probing the positivity bounds, for which the contributions of dim-10 operators, not subject to the same bounds, are a potential source of contamination. On the other hand, a potential future high energy photon collider [55] could measure the reverse process $\gamma\gamma \rightarrow f\bar{f}$ for different fermion final states, and probe a wider range of operators and their associated positivity bounds. We leave the detailed analyses of these colliders to future studies.

Acknowledgement We thank Ying-Ying Li for useful discussions. JG is supported by the Cluster of Excellence “Precision Physics, Fundamental Interactions, and Structure of Matter” (PRISMA+ EXC 2118/1) funded by the German Research Foundation (DFG) within the German Excellence Strategy (Project ID 39083149). LTW is supported by the DOE grant DE-SC0013642. CZ is supported by IHEP under Contract No. Y7515540U1, and by National Natural Science Foundation of China (NSFC) under grant No. 12075256 and No. 12035008.

Appendix A

SM $e^-\gamma \rightarrow e^-\gamma$ in the forward limit: We perform an explicit calculation of the amplitude $\mathcal{M}(e^-\gamma \rightarrow e^-\gamma)$ in SM in the forward limit with massless electrons. Our calculation follow closely Sec 5.5 of Ref. [56]. The general amplitude is given by

$$i\mathcal{M} = -ie^2 \epsilon_\mu^*(k') \epsilon_\nu(k) \bar{u}(p') \left[\frac{\gamma^\mu (\not{p} + \not{k}) \gamma^\nu}{(p+k)^2} + \frac{\gamma^\nu (\not{p} - \not{k}') \gamma^\mu}{(p-k')^2} \right] u(p), \quad (\text{A1})$$

where p , k , p' and k' are the momenta of the ingoing e^- , γ and the outgoing e^- , γ , respectively, as shown in Figure 3. We assume that both e^- and γ have + helicity (right-handed). It can be shown that the results are the same for the other helicity configurations. To calculate the amplitude in the forward limit, it is most convenient to choose a particular reference frame and a basis for the spinors. We choose the initial (and final) momenta to be along the z -axis, as shown in Figure 4. The Dirac matrices are given by

$$\gamma^\mu = \begin{pmatrix} 0 & \sigma^\mu \\ \bar{\sigma}^\mu & 0 \end{pmatrix}, \quad \text{where } \sigma^\mu = (1, \vec{\sigma}), \quad \bar{\sigma}^\mu = (1, -\vec{\sigma}). \quad (\text{A2})$$

Since we have chosen e^- and γ to be right-handed, we have for the Dirac spinor

$$u(p) = \begin{pmatrix} 0 \\ u_R(p) \end{pmatrix} \quad \text{where } u_R(p) = u_R(p') = \sqrt{2E} \begin{pmatrix} 0 \\ 1 \end{pmatrix}, \quad (\text{A3})$$

following the spinor choice in Ref. [56]. This also gives

$$\bar{u}(p') \gamma^\mu = u^\dagger(p') \gamma^0 \gamma^\mu = (0 \ u_R^\dagger(p) \sigma^\mu). \quad (\text{A4})$$

² “When you have excluded the impossible, whatever remains, however improbable, must be the truth.” – Sherlock Holmes

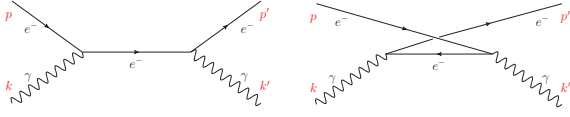


FIG. 3: Feynman diagrams for $e^- \gamma \rightarrow e^- \gamma$ in the SM.

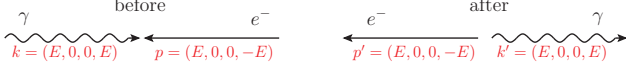


FIG. 4: Momenta of the forward scattering process before and after the collision.

The polarization vector are given by

$$\epsilon^\mu = \frac{1}{\sqrt{2}}(0, 1, i, 0)^\mu, \quad \epsilon^{*\mu} = \frac{1}{\sqrt{2}}(0, 1, -i, 0)^\mu, \quad (\text{A5})$$

which gives

$$\sigma^\mu \epsilon_\mu = \begin{pmatrix} 0 & -\sqrt{2} \\ 0 & 0 \end{pmatrix}, \quad \sigma^\mu \epsilon_\mu^* = \begin{pmatrix} 0 & 0 \\ -\sqrt{2} & 0 \end{pmatrix}. \quad (\text{A6})$$

Plugging everything into Equation A1, we have

$$\begin{aligned} \mathcal{M} &= -e^2 \epsilon_\mu^* \epsilon_\nu u_R^\dagger \left[\frac{\sigma^\mu \bar{\sigma} \cdot (p+k) \sigma^\nu}{s} + \frac{\sigma^\nu \bar{\sigma} \cdot (p-k') \sigma^\mu}{u} \right] u_R \\ &= -e^2 \epsilon_\mu^* \epsilon_\nu 2E (0 \ 1) \left[\begin{pmatrix} 0 & 0 \\ -\sqrt{2} & 0 \end{pmatrix} \frac{2E}{4E^2} \begin{pmatrix} 0 & -\sqrt{2} \\ 0 & 0 \end{pmatrix} + 0 \right] \begin{pmatrix} 0 \\ 1 \end{pmatrix} \\ &= -2e^2. \end{aligned} \quad (\text{A7})$$

Operators: Eq. A8 shows the five dimension-8 operators mentioned in the main text, as defined in Ref. [25]. The lepton flavor indices are omitted as they are not relevant for our study. The Lagrangian is written in the form $\mathcal{L}_{\text{dim-8}} = \sum_i \frac{c_i}{\Lambda^4} Q_i$.

$$\begin{aligned} Q_{l^2 B^2 D} &= i(\bar{l} \gamma^\mu \overleftrightarrow{D}^\nu l) B_{\mu\rho} B_\nu^\rho, \\ Q_{l^2 W B D}^{(2)} &= i(\bar{l} \gamma^\mu \tau^I \overleftrightarrow{D}^\nu l) (B_{\mu\rho} W_\nu^{I\rho} + B_{\nu\rho} W_\mu^{I\rho}), \\ Q_{l^2 W^2 D}^{(1)} &= i(\bar{l} \gamma^\mu \overleftrightarrow{D}^\nu l) W_{\mu\rho}^I W_\nu^{I\rho}, \\ Q_{e^2 B^2 D} &= i(\bar{e} \gamma^\mu \overleftrightarrow{D}^\nu e) B_{\mu\rho} B_\nu^\rho, \\ Q_{e^2 W^2 D} &= i(\bar{e} \gamma^\mu \overleftrightarrow{D}^\nu e) W_{\mu\rho}^I W_\nu^{I\rho}. \end{aligned} \quad (\text{A8})$$

Differential cross section: Figure 5 shows the differential cross section $d\sigma/d|\cos\theta|$ for the SM and the d8 contribution for $\sqrt{s} = 240$ GeV, unpolarized beams. The SM contribution dominates in the forward region due to the t/u -channel electron exchange.

Run scenarios: Table I is a summary of the run scenarios of future lepton colliders considered in our analysis, with the corresponding integrated luminosity. For ILC

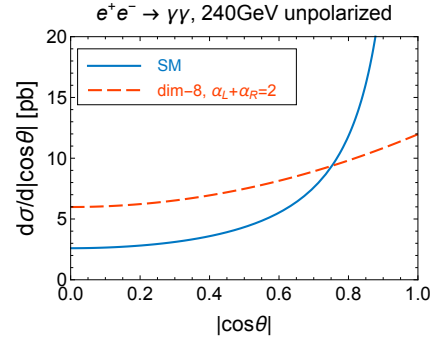


FIG. 5: The differential cross section $d\sigma/d|\cos\theta|$ for the SM and the d8 contribution (as in Eq. (4) in the main text) for $\sqrt{s} = 240$ GeV, unpolarized beams. For the d8 contribution, an arbitrary benchmark of $a_L + a_R = 2$ is chosen.

$\int \mathcal{L} dt$ [ab^{-1}]				
unpolarized	91 GeV	161 GeV	240 GeV	365 GeV
CEPC	8	2.6	5.6	
FCC-ee	150	10	5	1.5
ILC				
	250 GeV	350 GeV	500 GeV	
(-0.8, +0.3)	0.9	0.135	1.6	
(+0.8, -0.3)	0.9	0.045	1.6	
(±0.8, ±0.3)	0.1	0.01	0.4	
CLIC				
	380 GeV	1.5 TeV	3 TeV	
(-0.8, 0)	0.5	2	4	
(+0.8, 0)	0.5	0.5	1	
muon collider				
	10 TeV	30 TeV		
unpolarized	10	90		

TABLE I: A summary of the run scenarios of future lepton colliders considered in our analysis with the corresponding integrated luminosity.

and CLIC, the numbers in the brackets are the values of beam polarizations $P(e^-, e^+)$. For simplicity, we assume the Z -pole or WW -threshold runs are at one single energy. Numbers are taken from Refs. [28, 57]. Further details can be found in Refs. [35–38, 58, 59].

Measurement uncertainties: We have only considered statistical uncertainties in our analysis. Here we provide further verifications of this assumption. Figure 6 shows the total cross sections of diphoton process and the main background from Bhabha scattering ($e^+e^- \rightarrow e^+e^-$), the latter contributes to the diphoton channel if both final state particles mistagged as a photon. Even with a conservative 1% mistag rate for both electrons and positrons, this background is more than two orders of magnitude smaller than the signal. This is consistent with the LEP analysis in *e.g.* Ref. [60], which stated that the contamination from the major background, Bhabha events, was estimated to be less than 0.5% after selection cuts. Another potential source of background is the double-hard-FSR: $e^+e^- \rightarrow e^+e^- \gamma\gamma$,

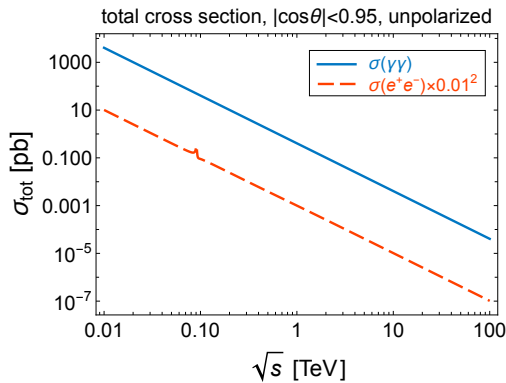


FIG. 6: The total cross sections of $e^+e^- \rightarrow \gamma\gamma$ and the main background from $e^+e^- \rightarrow e^+e^-$ with both final state particles mistagged as a photon. A cut on the production polar angle $|\cos\theta| < 0.95$ is applied. A conservative 1% mistag rate is assumed for both electrons and positrons.

where the two photons take most of the energy of the scattered electrons. Applying $m_{\gamma\gamma} \geq 0.9s$ on the invariant mass of the two photons with other reasonable cuts, we estimate the cross section of this process to be $6 \sim 7$ orders of magnitude lower than the signal process. The statistical uncertainties of the total diphoton cross section measurements are provided for each collider scenario in Table II as references.

$\Delta\sigma_{\text{tot}}/\sigma_{\text{tot}}, e^+e^- \rightarrow \gamma\gamma$				
unpolarized	91 GeV	161 GeV	240 GeV	365 GeV
CEPC	5.1×10^{-5}	1.6×10^{-4}	1.6×10^{-4}	
FCC-ee	1.2×10^{-5}	8.0×10^{-5}	1.7×10^{-4}	4.7×10^{-4}
ILC	250 GeV	350 GeV	500 GeV	
	2.5×10^{-4}	1.1×10^{-3}	3.7×10^{-4}	
CLIC	380 GeV	1.5 TeV	3 TeV	
	6.0×10^{-4}	1.5×10^{-3}	2.1×10^{-3}	
muon collider	10 TeV	30 TeV		
	5.0×10^{-3}	5.0×10^{-3}		

TABLE II: The projected (relative) statistical uncertainties of the total cross section measurement of $e^+e^- \rightarrow \gamma\gamma$ with the run scenarios in Table I. A cut on the production polar angle $|\cos\theta| < 0.95$ is applied.

* Electronic address: jiajin_gu@fudan.edu.cn

† Electronic address: liantaow@uchicago.edu

‡ Electronic address: cenzhang@ihep.ac.cn; corresponding author

- [1] A. Adams, N. Arkani-Hamed, S. Dubovsky, A. Nicolis, and R. Rattazzi, *Causality, analyticity and an IR obstruction to UV completion*, *JHEP* **10** (2006) 014, [[hep-th/0602178](#)].
 [2] B. Bellazzini, *Softness and amplitudes' positivity for*

spinning particles, *JHEP* **02** (2017) 034, [[arXiv:1605.06111](#)].

- [3] C. de Rham, S. Melville, A. J. Tolley, and S.-Y. Zhou, *Positivity bounds for scalar field theories*, *Phys. Rev. D* **96** (2017), no. 8 081702, [[arXiv:1702.06134](#)].
 [4] C. de Rham, S. Melville, A. J. Tolley, and S.-Y. Zhou, *UV complete me: Positivity Bounds for Particles with Spin*, *JHEP* **03** (2018) 011, [[arXiv:1706.02712](#)].
 [5] V. Chandrasekaran, G. N. Remmen, and A. Shahbazi-Moghaddam, *Higher-Point Positivity*, *JHEP* **11** (2018) 015, [[arXiv:1804.03153](#)].
 [6] C. de Rham, S. Melville, A. J. Tolley, and S.-Y. Zhou, *Positivity Bounds for Massive Spin-1 and Spin-2 Fields*, *JHEP* **03** (2019) 182, [[arXiv:1804.10624](#)].
 [7] B. Bellazzini and F. Riva, *New phenomenological and theoretical perspective on anomalous ZZ and Zγ processes*, *Phys. Rev. D* **98** (2018), no. 9 095021, [[arXiv:1806.09640](#)].
 [8] Q. Bi, C. Zhang, and S.-Y. Zhou, *Positivity constraints on aQGC: carving out the physical parameter space*, *JHEP* **06** (2019) 137, [[arXiv:1902.08977](#)].
 [9] G. N. Remmen and N. L. Rodd, *Consistency of the Standard Model Effective Field Theory*, *JHEP* **12** (2019) 032, [[arXiv:1908.09845](#)].
 [10] G. N. Remmen and N. L. Rodd, *Flavor Constraints from Unitarity and Analyticity*, [arXiv:2004.02885](#).
 [11] C. Zhang and S.-Y. Zhou, *A convex geometry perspective to the (SM)EFT space*, [arXiv:2005.03047](#).
 [12] B. Fuks, Y. Liu, C. Zhang, and S.-Y. Zhou, *Positivity in electron-positron scattering: testing the axiomatic quantum field theory principles and probing the existence of UV states*, [arXiv:2009.02212](#).
 [13] K. Yamashita, C. Zhang, and S.-Y. Zhou, *Elastic positivity vs extremal positivity bounds in SMEFT: a case study in transversal electroweak gauge-boson scatterings*, [arXiv:2009.04490](#).
 [14] S. Alioli, R. Boughezal, E. Mereghetti, and F. Petriello, *Novel angular dependence in Drell-Yan lepton production via dimension-8 operators*, *Phys. Lett. B* **809** (2020) 135703, [[arXiv:2003.11615](#)].
 [15] I. Low, R. Rattazzi, and A. Vichi, *Theoretical Constraints on the Higgs Effective Couplings*, *JHEP* **04** (2010) 126, [[arXiv:0907.5413](#)].
 [16] A. Falkowski, S. Rychkov, and A. Urbano, *What if the Higgs couplings to W and Z bosons are larger than in the Standard Model?*, *JHEP* **04** (2012) 073, [[arXiv:1202.1532](#)].
 [17] B. Bellazzini, L. Martucci, and R. Torre, *Symmetries, Sum Rules and Constraints on Effective Field Theories*, *JHEP* **09** (2014) 100, [[arXiv:1405.2960](#)].
 [18] J. Gu and L.-T. Wang, *Sum Rules in the Standard Model Effective Field Theory from Helicity Amplitudes*, *JHEP* **03** (2021) 149, [[arXiv:2008.07551](#)].
 [19] G. N. Remmen and N. L. Rodd, *Signs, Spin, SMEFT: Positivity at Dimension Six*, [arXiv:2010.04723](#).
 [20] H. Elvang and Y.-t. Huang, *Scattering Amplitudes*, [arXiv:1308.1697](#).
 [21] L. J. Dixon, *A brief introduction to modern amplitude methods*, in *Theoretical Advanced Study Institute in Elementary Particle Physics: Particle Physics: The Higgs Boson and Beyond*, pp. 31–67, 2014. [arXiv:1310.5353](#).
 [22] C. Cheung, *TASI Lectures on Scattering Amplitudes*, in *Proceedings, Theoretical Advanced Study Institute in*

- Elementary Particle Physics : Anticipating the Next Discoveries in Particle Physics (TASI 2016): Boulder, CO, USA, June 6-July 1, 2016*, pp. 571–623, 2018. [arXiv:1708.03872](#).
- [23] T. Ma, J. Shu, and M.-L. Xiao, *Standard Model Effective Field Theory from On-shell Amplitudes*, [arXiv:1902.06752](#).
- [24] G. Durieux and C. S. Machado, *Enumerating higher-dimensional operators with on-shell amplitudes*, *Phys. Rev. D* **101** (2020), no. 9 095021, [[arXiv:1912.08827](#)].
- [25] C. W. Murphy, *Dimension-8 operators in the Standard Model Effective Field Theory*, *JHEP* **10** (2020) 174, [[arXiv:2005.00059](#)].
- [26] H.-L. Li, Z. Ren, J. Shu, M.-L. Xiao, J.-H. Yu, and Y.-H. Zheng, *Complete Set of Dimension-8 Operators in the Standard Model Effective Field Theory*, [arXiv:2005.00008](#).
- [27] A. Azatov, R. Contino, C. S. Machado, and F. Riva, *Helicity selection rules and noninterference for BSM amplitudes*, *Phys. Rev. D* **95** (2017), no. 6 065014, [[arXiv:1607.05236](#)].
- [28] J. De Blas, G. Durieux, C. Grojean, J. Gu, and A. Paul, *On the future of Higgs, electroweak and diboson measurements at lepton colliders*, *JHEP* **12** (2019) 117, [[arXiv:1907.04311](#)].
- [29] M. Jiang, J. Shu, M.-L. Xiao, and Y.-H. Zheng, *New Selection Rules from Angular Momentum Conservation*, [arXiv:2001.04481](#).
- [30] B. Grzadkowski, M. Iskrzynski, M. Misiak, and J. Rosiek, *Dimension-Six Terms in the Standard Model Lagrangian*, *JHEP* **10** (2010) 085, [[arXiv:1008.4884](#)].
- [31] **ACME** Collaboration, V. Andreev et al., *Improved limit on the electric dipole moment of the electron*, *Nature* **562** (2018), no. 7727 355–360.
- [32] **Muon (g-2)** Collaboration, G. Bennett et al., *An Improved Limit on the Muon Electric Dipole Moment*, *Phys. Rev. D* **80** (2009) 052008, [[arXiv:0811.1207](#)].
- [33] K. Agashe, P. Du, S. Hong, and R. Sundrum, *Flavor Universal Resonances and Warped Gravity*, *JHEP* **01** (2017) 016, [[arXiv:1608.00526](#)].
- [34] **ALEPH, DELPHI, L3, OPAL, LEP Electroweak** Collaboration, S. Schael et al., *Electroweak Measurements in Electron-Positron Collisions at W-Boson-Pair Energies at LEP*, *Phys. Rept.* **532** (2013) 119–244, [[arXiv:1302.3415](#)].
- [35] **CEPC Study Group** Collaboration, M. Dong et al., *CEPC Conceptual Design Report: Volume 2 - Physics \mathcal{E} Detector*, [arXiv:1811.10545](#).
- [36] **FCC** Collaboration, A. Abada et al., *FCC Physics Opportunities: Future Circular Collider Conceptual Design Report Volume 1*, *Eur. Phys. J. C* **79** (2019), no. 6 474.
- [37] **FCC** Collaboration, A. Abada et al., *FCC-ee: The Lepton Collider: Future Circular Collider Conceptual Design Report Volume 2*, *Eur. Phys. J. ST* **228** (2019), no. 2 261–623.
- [38] P. Bambade et al., *The International Linear Collider: A Global Project*, [arXiv:1903.01629](#).
- [39] C. Hays, A. Martin, V. Sanz, and J. Setford, *On the impact of dimension-eight SMEFT operators on Higgs measurements*, *JHEP* **02** (2019) 123, [[arXiv:1808.00442](#)].
- [40] A. Crivellin, M. Hoferichter, and P. Schmidt-Wellenburg, *Combined explanations of $(g-2)_{\mu,e}$ and implications for a large muon EDM*, *Phys. Rev. D* **98** (2018), no. 11 113002, [[arXiv:1807.11484](#)].
- [41] M. Abe et al., *A New Approach for Measuring the Muon Anomalous Magnetic Moment and Electric Dipole Moment*, *PTEP* **2019** (2019), no. 5 053C02, [[arXiv:1901.03047](#)].
- [42] **Muon g-2** Collaboration, G. Bennett et al., *Final Report of the Muon E821 Anomalous Magnetic Moment Measurement at BNL*, *Phys. Rev. D* **73** (2006) 072003, [[hep-ex/0602035](#)].
- [43] **Particle Data Group** Collaboration, P. Zyla et al., *Review of Particle Physics*, *PTEP* **2020** (2020), no. 8 083C01.
- [44] **Muon g-2** Collaboration, B. Abi et al., *Measurement of the Positive Muon Anomalous Magnetic Moment to 0.46 ppm*, *Phys. Rev. Lett.* **126** (2021), no. 14 141801, [[arXiv:2104.03281](#)].
- [45] G. Gounaris, J. Layssac, and F. Renard, *Signatures of the anomalous Z_γ and ZZ production at the lepton and hadron colliders*, *Phys. Rev. D* **61** (2000) 073013, [[hep-ph/9910395](#)].
- [46] C. Degrande, *A basis of dimension-eight operators for anomalous neutral triple gauge boson interactions*, *JHEP* **02** (2014) 101, [[arXiv:1308.6323](#)].
- [47] J. Ellis, S.-F. Ge, H.-J. He, and R.-Q. Xiao, *Probing the scale of new physics in the $ZZ\gamma$ coupling at e^+e^- colliders*, *Chin. Phys. C* **44** (2020), no. 6 063106, [[arXiv:1902.06631](#)].
- [48] J. Ellis, H.-J. He, and R.-Q. Xiao, *Probing new physics in dimension-8 neutral gauge couplings at e^+e^- colliders*, *Sci. China Phys. Mech. Astron.* **64** (2021), no. 2 221062, [[arXiv:2008.04298](#)].
- [49] A. Azatov, J. Elias-Miro, Y. Reyimuaji, and E. Venturini, *Novel measurements of anomalous triple gauge couplings for the LHC*, *JHEP* **10** (2017) 027, [[arXiv:1707.08060](#)].
- [50] G. Panico, F. Riva, and A. Wulzer, *Diboson Interference Resurrection*, *Phys. Lett. B* **776** (2018) 473–480, [[arXiv:1708.07823](#)].
- [51] **LCC Physics Working Group** Collaboration, K. Fujii et al., *Implications of the 750 GeV gamma-gamma Resonance as a Case Study for the International Linear Collider*, [arXiv:1607.03829](#).
- [52] K. Aoki, S. Mukohyama, and R. Namba, *Positivity vs. Lorentz-violation: an explicit example*, [arXiv:2107.01755](#).
- [53] R. Contino, A. Falkowski, F. Goertz, C. Grojean, and F. Riva, *On the Validity of the Effective Field Theory Approach to SM Precision Tests*, *JHEP* **07** (2016) 144, [[arXiv:1604.06444](#)].
- [54] S. Alte, M. König, and W. Shepherd, *Consistent Searches for SMEFT Effects in Non-Resonant Dijet Events*, *JHEP* **01** (2018) 094, [[arXiv:1711.07484](#)].
- [55] **ALEGRO** Collaboration, E. Adli et al., *Towards an Advanced Linear International Collider*, [arXiv:1901.10370](#).
- [56] M. E. Peskin and D. V. Schroeder, *An Introduction to quantum field theory*. Addison-Wesley, Reading, USA, 1995.
- [57] T. Han, D. Liu, I. Low, and X. Wang, *Electroweak Couplings of the Higgs Boson at a Multi-TeV Muon Collider*, [arXiv:2008.12204](#).

- [58] J. de Blas, R. Franceschini, F. Riva, P. Roloff, U. Schnoor, M. Spannowsky, J. Wells, A. Wulzer, J. Zupan, et al., *The CLIC Potential for New Physics*, [arXiv:1812.02093](#).
- [59] J. P. Delahaye, M. Diemoz, K. Long, B. Mansoulié, N. Pastrone, L. Rivkin, D. Schulte, A. Skrinsky, and A. Wulzer, *Muon Colliders*, [arXiv:1901.06150](#).
- [60] **L3** Collaboration, M. Acciarri et al., *Tests of QED at LEP energies using $e^+ e^- \rightarrow \gamma \gamma$ ($\gamma \gamma$) and $e^+ e^- \rightarrow \text{lepton}^+ \text{lepton}^- \gamma \gamma$* , *Phys. Lett. B* **353** (1995) 136–144.